Synthesis and Characterization of Mg–Al–CO3 Layered Double Hydroxide for CO2 Adsorption

ARTICLE *in* INDUSTRIAL & ENGINEERING CHEMISTRY RESEARCH · NOVEMBER 2008

Impact Factor: 2.59 · DOI: 10.1021/ie800365t

3 AUTHORS, INCLUDING:

Beena Tyagi
Central Salt and Marine Chemicals Researc…
47 PUBLICATIONS **926** CITATIONS
SEE PROFILE

Raksh Vir Jasra
Reliance Industries Limited
328 PUBLICATIONS **5,523** CITATIONS
SEE PROFILE

Synthesis and Characterization of Mg−Al−CO_3 Layered Double Hydroxide for CO_2 Adsorption

Ulka Sharma, Beena Tyagi, and Raksh. V. Jasra*,†

Discipline of Inorganic Materials & Catalysis, Central Salt & Marine Chemicals Research Institute, G. B. Marg, Bhavnagar 364 002, Gujarat, and R & D Centre, Reliance Industries Limited, Vadodara Manufacturing Division, Vadodara 391346, India

A series of Mg−Al−CO_3 layered double hydroxide (LDH) samples have been synthesized by conventional precipitation and coprecipitation methods. The effect of various synthetic parameters, such as cation molar ratio, mode of addition of magnesium and aluminum precursors, addition temperature, agitation, and drying conditions, on the structural, textural, and thermal behavior of the samples has been studied. These properties were correlated with the CO_2 adsorption capacity of the samples. The Mg−Al−CO_3 LDH sample prepared with optimized synthetic parameters has shown the higher CO_2 adsorption capacity (22 cm^3/g).

1. Introduction

Layered double hydroxides (LDHs), also known as synthetic anionic clays or hydrotalcite-like compounds (HTlcs), consist of stacked layers of brucite [$Mg(OH)_2$] having some of its divalent cations (Mg^{2+}) substituted by trivalent cations (Al^{3+}) at the centers of octahedral sites of the hydroxide sheet whose vertex contains hydroxide ions that are shared by three octahedral cations and point toward the interlayer region. Positively charged layers can be balanced by the exchangeable interlayer anions.[1−4] LDHs are represented by the general formula $[M^{II}_{1-x}M^{III}_x(OH)_2]^{x+}A^{n-}_{x/n}\cdot mH_2O$, where M^{II} is a divalent cation (Mg^{2+} and/or Ni^{2+}, Zn^{2+}, Co^{2+}), M^{III} is a trivalent cation (Al^{3+} and/or Fe^{3+}, Ga^{3+}, Cr^{3+}), and A is an anion with charge n (OH^-, CO_3^{2-}, NO_3^-, Cl^-, SO_4^{2-}).[5−7] x is $M^{III}/M^{II}+M^{III}$ and is normally between 0.17 and 0.33; however, LDH with significantly higher x values has also been reported.[8,9]

LDHs possess a well-defined layered structure (Figure 1) with unique properties such as adsorption capacity, anion exchange capacity, and mobility of interlayer anions and water molecules. On thermal decomposition, LDH's form stable and homogeneous mixed oxides and have the ability to reconstruct their structure when exposed to water and carbon dioxide. These materials have been widely studied as adsorbents for gas molecules[10−13] and liquid ions[14−16] and as catalysts and catalyst support.[17−20] One of the potential applications of these materials includes adsorption of CO_2 at high temperature. The removal and recovery of CO_2 from hot gas stream is becoming increasingly significant in the field of ecofriendly energy production. The combustion of fossil fuels such as coal or natural gas releases large volumes of CO_2 into the environment, resulting into pollution problem. Studies of CO_2 adsorption on LDHs suggest that these materials have the attributes of a good adsorbent, such as high adsorption selectivity and capacity, adequate adsorption/desorption kinetics at operating conditions, and mechanical strength of adsorbent particles after cyclic exposure to high-pressure streams.[5,21−26] However, the adsorption capacity of these materials is significantly influenced by their structural, textural, and thermal behavior, which is further determined by the synthetic parameters. In general, higher x values results into higher adsorption capacity,[13] but an optimum amount of Al content is found necessary for maximum adsorption. For example, by decreasing the Al content in Mg−Al-LDH from 70% to 50%, CO_2 adsorption was found to increase from 0.368 to 0.42 mmol/g at 300 °C temperature and 1 bar pressure; however, a further decrease in Al content to 30% resulted in a decrease of the CO_2 adsorption capacity to 0.26 mmol/g.[26] Modification with alkali salts such as K_2CO_3 increased both the adsorption capacity and the stability of the LDHs.[27,28] Addition of rare earth elements has also enhanced the adsorption capacity.[29] The amount of CO_2 adsorption is also affected by the interlayer spacing, the size, and charge density of the intercalated anion. Several studies have been carried out on the synthesis of Mg−Al LDH and other LDHs using different methods such as conventional precipitation, sol−gel and urea hydrolysis,[30−33] and thermal decomposition.[34−38] CO_2 adsorption studies on LDHs have been reported[25−29,39−44] in the literature. However, none of the studies referred to above have covered the optimization of synthetic parameters for improving the adsorption capacity of LDH and the effect of synthetic parameters on CO_2 adsorption capacity of LDH.

In the present study, a series of Mg−Al−CO_3 LDH samples have been synthesized with precipitation and coprecipitation method with varied synthetic parameters, namely, magnesium and aluminum cation molar ratio, mode of magnesium and aluminum precursors addition, addition temperature, agitation, and drying conditions. The effect of the synthetic parameters on the structural, textural, and thermal behavior of the samples has been studied and correlated with their CO_2 adsorption capacity.

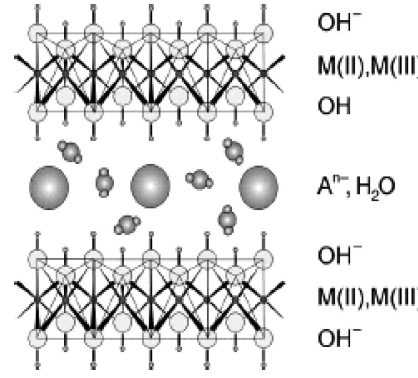

Figure 1. Structure of layered double hydroxide.

* To whom correspondence should be addressed. Tel: +91265-6693935. Fax: +91-265-6693934.

† Reliance Industries Limited.

10.1021/ie800365t CCC: $40.75
Published on Web 11/06/2008

Table 1. Synthesis of Mg−Al−CO_3 LDH Samples with Varied Synthetic Parameter

sample	Mg:Al molar ratio	mode of addition	temperature (°C)			yield (%)[a]
			addition	agitation	drying	
Mg−Al-1	1.7:1	precipitation	65	65	30	79
Mg−Al-2	2:1	precipitation	65	65	30	79
Mg−Al-3	3:1	precipitation	65	65	30	74
Mg−Al-4	1.7:1	coprecipitation	65	65	30	69
Mg−Al-5	1.7:1	coprecipitation	65	65	110	68
Mg−Al-6	1.7:1	coprecipitation	65		110	52
Mg−Al-7	1.7:1	coprecipitation	30		110	62
Mg−Al-8	1.7:1	coprecipitation	30		30	66
Mg−Al-9	1.7:1	coprecipitation	30	65	30	52

[a] The yield of Mg−Al−CO_3 LDH samples was calculated as yield (wt %) = (obtained weight of product/theoretical weight of product) × 100.

2. Materials and Methods

Magnesium nitrate was procured from s.d. Fine Chem. Ltd., aluminum nitrate was from LOBA Chemie Pvt. Ltd., sodium carbonate was from National Chemicals, and sodium hydroxide was procured from Ranbaxy, Ltd. Commercial hydrotalcite (PMG63) was obtained from Sasol GmbH (Hamburg, Germany). All chemicals were used as such. CO_2 gas (99.92% purity) was from Inox Air Product Ltd., India.

2.1. Synthesis of Mg−Al−CO_3 LDHs. A series of Mg−Al−CO_3 LDH samples were synthesized by conventional precipitation and coprecipitation methods. Solutions of three different cation molar ratios, i.e., 1.7:1, 2:1, and 3:1, have been prepared as below.

Solution A was prepared by dissolving Mg and Al nitrate salts with different molar concentration such as $[Mg(NO_3)_2]$ = 0.63 M, $[Al(NO_3)_3]$ = 0.37 M for Mg:Al = 1.7:1; $[Mg(NO_3)_2]$ = 0.66 M, $[Al(NO_3)_3]$ = 0.34 M for Mg:Al = 2:1; and $[Mg(NO_3)_2]$ = 0.75 M and $[Al(NO_3)_3]$ = 0.25 M for Mg:Al = 3:1. For different molar concentration ratio of Mg and Al, the x value is 0.37, 0.34, and 0.25 for 1.7:1, 2:1, and 3:1, respectively, where x = Al/Al + Mg.

Solution B having sodium carbonate [Na_2CO_3:$Mg(NO_3)_2$ = 1:1 molar ratio] dissolved in 100 mL of NaOH (2.2 M) was prepared separately. Addition of solution A and solution B was done in two different ways.

2.1.1. Precipitation Method (Precipitation at Variable pH). Solution A was slowly added to solution B at the flow rate of 0.5−1.0 mL min^{-1}. The samples obtained with different Mg:Al ratios were designated as Mg−Al-1 to Mg−Al-3. This method is defined as precipitation at variable pH, because when solution A (acidic) is added to solution B (basic), the pH of the resultant solution will be changed and the pH will be variable during the precipitation process.

2.1.2. Coprecipitation Method (Precipitation at Constant pH). Both solutions A and B were added into a container simultaneously at a flow rate of 8−10 mL min^{-1}. This method is defined as precipitation at constant pH, because when a basic and an acidic solution having similar molarities are added simultaneously to a common container with same flow rate, the pH of resultant solution will be constant during the precipitation process.

A series of samples having Mg:Al molar ratio 1.7:1 (x = 0.37) were prepared under different synthetic parameters such as addition temperature, agitation, drying temperature, and pH as shown in Table 1. The samples obtained are designated as Mg−Al-4 to Mg−Al-9. The chemical compositions of LDH prepared with different Mg:Al molar ratio are given in Table 2.

2.2. Characterization. 2.2.1. Powder X-Ray Diffraction Studies (PXRD). The d spacing and crystallinity of LDH samples were measured by X-ray powder diffractometer (Philips X'pert) using Cu Kα radiation (λ = 1.5405Å). The samples were scanned in 2θ range from 0° to 70° at a scanning rate of 0.4° s^{-1}. Crystallite size, i.e., disk diameter, was calculated for the 003 reflection (2θ = 11.6) using the Scherrer formula[45] with a shape factor (K) of 0.9 as below:

$$\text{crystallite size} = K\lambda/W\cos\theta$$

where $W = W_b - W_s$ and W_b = broadened profile width of experimental sample and W_s = standard profile width of reference silicon sample. Lattice parameters of Mg−Al−CO_3 LDH samples were compared with the reference hydrotalcite samples using JCPDS files.

In situ high-temperature powder X-ray diffraction (HT-PXPD) measurements were done in the temperature range from 200 to 500 °C with a heating rate of 20 °C min^{-1} using an XRK reactor chamber to determine the structural modifications of LDH samples during heating.

2.2.2. Thermal Gravimetric Analysis. TG/DTA analysis of LDH samples was performed using TGA (Mettler Toledo Star^e System) in the temperature range from 50 to 750 °C with a heating rate of 10 °C min^{-1} under N_2 flow (40 cm^3 min^{-1}).

2.2.3. Surface Area Analysis. N_2 adsorption and desorption isotherms of various LDH samples were measured at 77.4 K using an ASAP 2010 Micromeritics instrument. Prior to measurement, the samples were activated in situ by heating at 150 °C under vacuum (1×10^{-3} mmHg) for 2 h. Surface area was determined from N_2 adsorption data using the BET equation.[46]

2.2.4. Chemical Analysis. The elemental analysis of Mg and Al in the synthesized LDH samples was carried out using inductivity coupled plasma (ICP) emission spectroscopy with a Perkin-Elmer Optima 2000 DV optical emission spectrometer. The solution used for the analysis was prepared by dissolving 4 ppm (for magnesium) and 10 ppm (for aluminum) of LDH samples in 5% HNO_3. The total water content of LDH sample has been analyzed by a Karl Fischer titrator (TitraMaster 85) and also calculated on the basis of weight loss observed during TG analysis. The water content was found to be in the range of 0.44−0.58 mol/mol of LDH by Karl Fischer titrator; however, theoretically calculated values are in the range of 0.52−0.76 mol/mol of LDH. The values obtained by Karl Fischer titrator included in the molecular formula of LDH sample are shown in Table 2.

2.2.5. CO_2 Adsorption−Desorption Study. CO_2 adsorption and desorption measurements were carried out in LDH samples using an ASAP 2010 Micromeritics instrument. CO_2 adsorption isotherms were measured at 30 and 60 °C up to 1 bar equilibrium pressure. Prior to adsorption measurements, the samples were activated in situ by heating at 150 °C under vacuum (1×10^{-3} mmHg) for 2 h. The effect of activation temperatures (250 and 350 °C) on CO_2 adsorption isotherms was also studied. The error in adsorption measurements was calculated to be in the range of ±0.2%.

The measured adsorption isotherms were fitted into Langmuir,[47] Freundlich,[48] and Langmuir−Freundlich[47] isotherm models given below

$$\frac{q}{q_m} = \frac{bp}{1+bp} \quad (1)$$

$$q = KP^n \quad (2)$$

$$\frac{q}{q_m} = \frac{bp^n}{1+bp^n} \quad (3)$$

Table 2. Characterization of Mg−Al−CO_3 LDH Samples

sample	d_{003} (nm)	003 disk diameter (nm)	lattice strain (%)	surface area (m^2/g)	CO_2 adsorption (cm^3/g)	formula
Mg−Al-1	0.762	35	1.366	65	14.8	$Mg_{0.63}Al_{0.37}(OH)_2(CO_3)_{0.185}0.51H_2O$
Mg−Al-2	0.764	32	1.454	65	12.0	$Mg_{0.67}Al_{0.33}(OH)_2(CO_3)_{0.165}0.44\ H_2O$
Mg−Al-3	0.778	11	3.535	71	8.0	$Mg_{0.75}Al_{0.25}(OH)_2(CO_3)_{0.125}0.52H_2O$
Mg−Al-4	0.761	43	1.161	67	16.2	$Mg_{0.63}Al_{0.37}(OH)_2(CO_3)_{0.185}\ 0.57H_2O$
Mg−Al-5	0.760	38	1.268	74	13.2	$Mg_{0.63}Al_{0.37}(OH)_2(CO_3)_{0.185}\ 0.55H_2O$
Mg−Al-6	0.763	13	2.978	34	10.0	$Mg_{0.63}Al_{0.37}(OH)_2(CO_3)_{0.185}\ 0.45H_2O$
Mg−Al-7	0.760	12	3.326	44	12.0	$Mg_{0.63}Al_{0.37}(OH)_2(CO_3)_{0.185}0.44H_2O$
Mg−Al-8	0.763	10	4.006	29	14.2	$Mg_{0.63}Al_{0.37}(OH)_2(CO_3)_{0.185}0.51H_2O$
Mg−Al-9	0.760	51	1.034	65	22.0	$Mg_{0.63}Al_{0.37}(OH)_2(CO_3)_{0.185}0.58H_2O$
Mg−Al−C					16.0	
PMG63	0.763				22.0	$Mg_{0.63}Al_{0.37}(OH)_2(CO_3)_{0.185}0.58H_2O$

Table 3. Lattice Parameters of Mg−Al−CO_3 LDH Samples

	lattice parameters (nm)				
sample	*a*	*c*	crystal type	polytype	reference
Mg−Al-1	0.6120	1.5324	hexagonal	two layer (2H)	manasseite (JCPDS-14-525)
Mg−Al-2	0.6200	4.6855	rhombohedral	six layer (6R)	hydrotalcite, syn (JCPDS-22-700)
Mg−Al-3	0.3070	2.3230	rhombohedral	three layer (3R)	hydrotalcite (JCPDS-14-191)
Mg−Al-4	0.6200	4.6855	rhombohedral	six layer (6R)	hydrotalcite, syn (JCPDS-22-700)
Mg−Al-9	0.6200	4.6855	rhombohedral	six layer (6R)	hydrotalcite, syn (JCPDS-22-700)
Mg−O[a]	0.4211		cubic		periclase, syn (JCPDS-45-946)

[a] Sample after in situ heat treatment at 400 and 500 °C during HT-PXRD.

where q is the amount of gas adsorbed by the adsorbent at equilibrium, q_m is the monolayer or saturated amount adsorbed, b is the Langmuir constant, and P is the equilibrium pressure of the adsorbate. The quantity $q_m b$ equals K. K and n are fitting parameters.

3. Results and Discussion

3.1. Structural Properties. 3.1.1. Powder X-Ray Diffraction Studies. Powder X-Ray diffractograms of Mg−Al−CO_3 LDH samples given in Figure 2a show the structure of hydrotalcite (JCPDS-14-191) displaying the characteristic reflections: (i) sharp and intense basal 00*l* reflections of 003 and 006 planes in the low angle region ($2\theta < 25°$), (ii) broad 0*kl* reflections of 012, 015, and 018 planes in the middle angle region ($2\theta = 30°-50°$), and (iii) sharp *hk*0 and *hkl* reflections of 110, 113, and 116 planes in the high angle region ($2\theta = 55°-65°$). The LDH samples synthesized under different synthetic parameters have similar structure; however, variation in interlayer *d*-spacing of characteristic 003 planes (d_{003}), crystallinity, and other structural features were observed to be affected by synthetic parameters as shown in Table 2 and briefly discussed below.

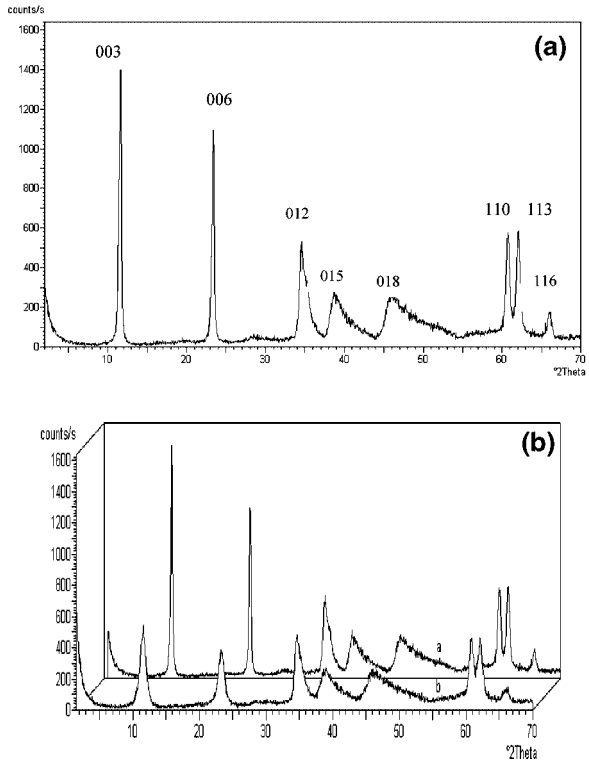

Figure 2. (a) XRD pattern of Mg−Al−CO_3 LDH. (b) XRD pattern of Mg−Al−CO_3 (a) with agitation and (b) without agitation.

3.1.1.1. Effect of Mg:Al Ratio. The d_{003}, crystallinity, and lattice strain were observed to decrease with increasing the Al content or x value. The theoretical value of d_{003} of Mg−Al−CO_3 is expected to be 0.760 nm, considering the thickness of the brucite-like layer to be 0.48 nm and the gallery height in CO_3^{2-} containing LDH being 0.28 nm.[7] LDH samples synthesized by the precipitation and coprecipitation method were found to have d_{003} values of 0.760−0.778 nm, depending upon the synthetic parameters. For example, d_{003} decreases from 0.778 to 0.762 nm with increasing the Al content from 25 to 37 mol % (Table 2). The lattice strain was also observed to decrease from 3.535 to 1.366 with increasing the Al content from 25 to 37 mol %, which results in the increase of the crystallite size, i.e., disk diameter increases from 11 to 35 nm (Table 3). It may be noted that, for layered materials such as LDHs, crystallite size is defined along the $a-b$ plane as disk diameter.[49] In the samples having higher Al content, the smaller size of Al^{3+} (0.50 Å) as compared to Mg^{2+} (0.65 Å) leads to significant decrease in the lattice strain and also in d_{003} value.

LDH sample having an Al content of 37 mol % was observed to show maximum CO_2 adsorption at 150 °C and 1 bar (discussed in later section); therefore, for the present study, LDH with 37 mol % Al content, i.e., 1.7:1 Mg:Al molar ratio, was chosen as the optimum cation molar ratio for preparing different LDH samples.

3.1.1.2. Effect of Mode of Addition of Precursor. LDH samples prepared by coprecipitation mode (i.e., precipitation at constant pH) showed higher CO_2 adsorption capacity (16.2 cm^3/g) as compared to LDH samples prepared by precipitation mode (i.e., precipitation at variable pH) (14.8 cm^3/g), all other

parameters being similar. Therefore, the coprecipitation method was chosen to prepare other LDH samples with varied synthetic parameters.

3.1.1.3. Effect of Agitation. Among the various synthetic parameters, agitation of the precipitated sample was observed to have significant effect on the crystallinity and disk diameter of LDH sample, without affecting much the d_{003} value. For example, LDH samples prepared without agitation (Mg−Al-6 to Mg−Al-8) were found to be less crystalline, having lower disk diameter (10−13 nm, Table 2) as compared to samples prepared with agitation (Mg−Al-4, Mg−Al-5, and Mg−Al-9), which had higher crystallinity (Figure 2b) and higher disk diameter (38−51 nm). However, the d_{003} value was observed in the range of 0.760−0.763 nm.

3.1.1.4. Effect of Addition and Drying Temperature. Among the two temperatures (room temperature, i.e., 30, and 65 °C; Table 1) studied during the addition of solutions A and B, room temperature addition slightly favors the crystallinity. Similarly, drying of LDH sample at room temperature for 24 h enhanced the crystallinity of the sample as compared to oven drying at 110 °C for 12 h, whereas the d_{003} value remains in a similar range. Similar observations that the lower temperature is more effective for the formation of HTs with high Al^{3+} substitution have been reported[22] earlier.

On the basis of the above results on various synthetic parameters, coprecipitation of solutions A (having 37 mol % Al) and B at room temperature followed by agitation of precipitated hydrotalcite at 65 °C for 18 h and drying at room temperature for 24 h were chosen as optimum synthetic parameters to prepare Mg−Al−CO_3 LDH. The sample prepared (Mg−Al-9) using these optimized synthetic conditions was observed to be highly crystalline with $d_{003} = 0.760$ nm, the highest disk diameter of 51 nm, and the highest CO_2 adsorption capacity, 22 cm^3/g (Table 2).

3.1.1.5. Lattice Parameters. Table 3 shows the lattice parameters of some LDH samples, the XRD pattern of which was compared with the reference hydrotalcite of JCPDS files. It is interesting to note that LDH samples prepared with different Mg:Al molar ratios showed variation in a and c unit cell parameters, where a corresponds to the average metal−metal distance within the layer and c corresponds to layer-to-layer distance.[50] As the layered sheet of metal hydroxide can be stacked in various ways, a number of polytypes can be formed. In the present study, we have observed the formation of different polytypes, namely 2H, 3R, and 6R, by comparison with reference hydrotalcite as given in Table 3.

3.1.1.6. High-Temperature Powder X-ray Diffraction (HT-PXRD) Studies. To study the structural modification of hydrotalcite phase on heating, in situ heating of sample was carried out in the temperature range of 200−500 °C. Heating at 200−300 °C results in a significant decrease in the crystallinity and d_{003} (Figure 3) due to dehydration of interlayer water molecules and dehydroxylation. Further heating at 350 °C leads to dehydroxylation along with decarbonation, which results in the destruction of the layered structure of hydrotalcite, and formation of mixed oxide was observed to start. At 400 and 500 °C, the presence of cubic MgO was observed (JCPDS-45-946) having $a = 0.421$ nm and characteristic d-spacing of $d_{002} = 2.09$ and $d_{220} = 1.48$ at 43.1° and 62.6° 2θ, respectively.

3.1.2. Thermal Analysis. All prepared Mg−Al−CO_3 LDH samples showed the total weight loss in the range of 36−43%. The DTA curve showed two endothermic peaks, first a sharp peak at ∼200 °C (weight loss = 16%) due to dehydration of interlayer water and the second broad peak at ∼400 °C (weight loss = 24−27%) due to decarbonation (Figure 4a) The DTA curve after CO_2 adsorption (Figure 4b) showed increased weight loss of 4.5% during the decarboxylation and decarbonation, which was found similar to the weight increase after CO_2 adsorption (22 cm^3/g).

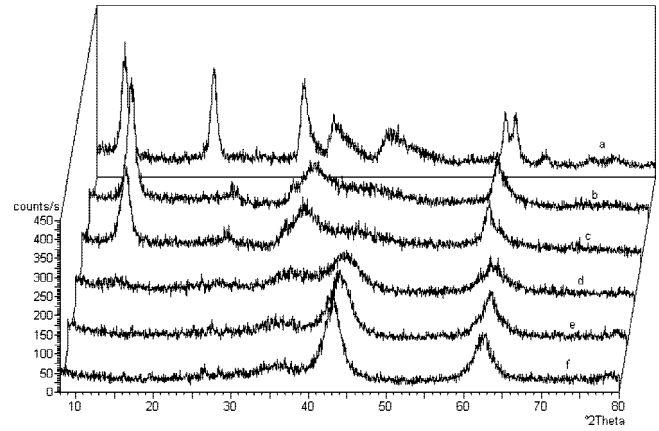

Figure 3. HT-XRD of Mg−Al−CO_3 LDH: d_{003} at (a) 25 °C = 0.778 nm, (b) 200 °C = 0.667 nm, (c) 300 °C = 0.655 nm, and (d) 350 °C = 0.653 nm, (e) 400 °C, (f) 500 °C.

3.2. CO_2 Adsorption Study. The adsorption isotherms of CO_2 on Mg−Al−CO_3 samples followed type III isotherm ($1/n < 1$). In type III isotherm with $1/n < 1$, the amount of gas adsorbed exponentially increases with increasing pressure. This is attributed to the formation of additional layers of physically adsorbed gas molecules.[47,48] The Langmuir, Freundlich, and Langmuir−Freundlich parameters for the CO_2 adsorption are given in Tables 4, 5, and 6, respectively. The parameters for CO_2 adsorption on Mg−Al-9 LDH sample at different activation and adsorption temperatures are given in Tables 7, 8, and 9. Figure 5 shows the isotherms of the experimental data and the isotherm model data for the adsorption of CO_2. The Langmuir isotherm fails to fit (variance = 0.432−3.384) with the experimental data in all the cases. The Langmuir−Freundlich isotherm gives a better fit (variance = 0.0647−0.7286), but the Freundlich isotherm gives an excellent fit (variance 0.0616−0.6844) with the experimental data. The Langmuir isotherm fails to fit with the experimental data because it represents monolayer chemisorption, whereas the experimental data shows multilayer adsorption having both chemisorption and physisorption, i.e., the adsorption up to the Langmuir saturation point shows chemisorption followed by physisorption.

The LDH samples were found to adsorb CO_2 in the range of 8−22 cm^3/g at 1 bar pressure and 30 °C. The study reveals that the CO_2 adsorption capacity of LDH can be enhanced by variation in synthetic conditions, as synthetic parameters were observed to have significant effect on the CO_2 adsorption capacity of LDH, which are briefly discussed as below.

The LDH samples having lower Al content (25 mol % and $x = 0.25$) showed a minimum CO_2 adsorption of 8 cm^3/g, which increased to 14.8 cm^3/g for the LDH samples having higher Al content (37 mol % and $x = 0.37$) (Figure 6a,b). This shows that increased charge density due to the presence of higher Al content leads to an increase in the basicity of the material. The enhanced basicity of hydrotalcite will further lead to an increase in chemisorption of acidic carbon dioxide, thus resulting in higher adsorption capacity for CO_2.

The correlation between Al content and CO_2 adsorption capacity by Langmuir saturation point indicates that with an increase in Al content, chemisorption also increases. For the minimum Al content studied (25 mol %), the volume of CO_2

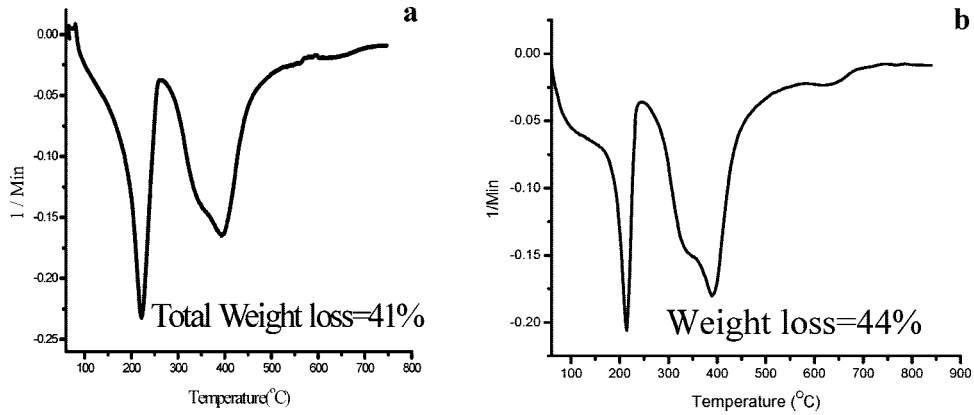

Figure 4. TG analysis of Mg−Al−CO_3 LDH: (a) before CO_2 adsorption and (b) after CO_2 adsorption.

Table 4. Langmuir Parameters for CO_2 Adsorption at 30 °C on Mg−Al−CO_3 LDH Samples

sample[a]	q ($cm^3\ g^{-1}$ $mmHg^{-1}$)	b ($mmHg^{-1}$)	regression (R^2)	variance
Mg−Al-1	13.965	0.0161	0.7679	1.690
Mg−Al-2	11.080	0.0231	0.7679	1.690
Mg−Al-3	7.341	0.0179	0.8509	0.432
Mg−Al-4	14.735	0.0301	0.7439	3.299
Mg−Al-5	13.331	0.0133	0.8466	1.508
Mg−Al-6	9.186	0.0142	0.8446	0.738
Mg−Al-7	10.291	0.0263	0.6796	2.309
Mg−Al-8	13.892	0.0149	0.8410	1.485
Mg−Al-9	18.208	0.0774	0.8540	3.384
Mg−Al−C	16.709	0.0046	0.9327	1.014
PMG63	87.080	0.0003	0.9745	0.820

[a] Activated at 150 °C under vacuum (1×10^{-3} mmHg), 2 h.

Table 5. Freundlich Parameters for CO_2 Adsorption at 30 °C on Mg−Al−CO_3 LDH Samples

sample[a]	K ($cm^3\ g^{-1}$ $mmHg^{-n}$)	n	regression (R^2)	variance
Mg−Al-1	2.709	0.2428	0.9788	0.2253
Mg−Al-2	2.656	0.2160	0.9712	0.2087
Mg−Al-3	1.537	0.2327	0.9787	0.0616
Mg−Al-4	4.034	0.7991	0.9689	0.4003
Mg−Al-5	2.294	0.2576	0.9773	0.2223
Mg−Al-6	1.576	0.2605	0.9751	0.1179
Mg−Al-7	2.793	0.1982	0.9655	0.2487
Mg−Al-8	2.676	0.2428	0.9799	0.1876
Mg−Al-9	6.104	0.1772	0.9814	0.4305
Mg−Al−C	0.866	0.4133	0.9906	0.1403
PMG63	0.059	0.8529	0.9787	0.6844

[a] Activated at 150 °C under vacuum (1×10^{-3} mmHg), 2 h.

Table 6. Langmuir−Freundlich Parameters for CO_2 Adsorption at 30 °C on Mg−Al−CO_3 LDH Samples

sample[a]	q ($cm^3\ g^{-1}$ $mmHg^{-n}$)	b ($mmHg^{-n}$)	n	regression (R^2)	variance
Mg−Al-1	808.97	0.0033	0.2458	0.9785	0.2373
Mg−Al-2	1010.98	0.0026	0.2177	0.9710	0.2184
Mg−Al-3	505.98	0.0030	0.2352	0.9784	0.0647
Mg−Al-4	1010.93	0.0039	0.2012	0.9685	0.4199
Mg−Al-5	808.95	0.0028	0.2604	0.9770	0.2339
Mg−Al-6	916.47	0.0017	0.2623	0.9749	0.1237
Mg−Al-7	1010.99	0.0027	0.1995	0.9651	0.2596
Mg−Al-8	1580.06	0.0016	0.2443	0.9797	0.1952
Mg−Al-9	520.83	0.0915	0.1860	0.9814	0.4464
Mg−Al−C	909.95	0.0009	0.4173	0.9904	0.1499
PMG63	404.98	0.0001	0.8726	0.9781	0.7286

[a] Activated at 150 °C under vacuum (1×10^{-3} mmHg), 2 h.

adsorbed by Langmuir saturation point is 5.32 cm^3/g, but for the 33 and 37 mol % Al content, the volume of CO_2 adsorbed is 9.47 and 10.97 cm^3/g, respectively. The amount of CO_2 adsorbed in terms of CO_3^{2-} content has also been calculated. In general, a 1 mol % increase in Al content results in an increase of CO_3^{2-} content by 0.5 mol.

Among the two modes of addition of solutions A and B, the LDH samples prepared with coprecipitation showed slightly higher CO_2 adsorption (16.2 cm^3/g) versus LDH samples prepared with the precipitation method (14.8 cm^3/g) (Figure 6c). It may be due to the higher crystallinity of the material formed at constant pH.

Agitation of the precipitated solution plays an important role in the CO_2 adsorption capacity of LDH. For example, LDH sample prepared with agitation showed higher CO_2 adsorption (13.5 cm^3/g) than the sample prepared without agitation, which showed lower CO_2 adsorption (10 cm^3/g), with other synthetic parameters similar (Figure 6d). Furthermore, the sample prepared by room temperature addition of the two solutions without agitation showed lower CO_2 adsorption (14.2 cm^3/g) than the sample prepared by addition at 65 °C with agitation (16.2 cm^3/g). Samples prepared through agitation are more crystalline as compared to samples prepared without agitation; the higher crystallinity of agitated samples increases the basicity of the material and thus results in an increase in the adsorption capacity for CO_2.

The temperature of addition of two solutions also affects the CO_2 adsorption. For example, LDH sample prepared at room temperature addition showed higher CO_2 adsorption (12 cm^3/g) as compared to sample prepared by addition at 65 °C, which shows lower CO_2 adsorption (10 cm^3/g) with other synthetic parameters being similar (Figure 6e). Room temperature addition favors the crystallinity (as discussed above) which increases the basic sites, thus resulting in enhanced adsorption capacity for CO_2 chemisorption.

Drying temperature is another parameter that influences the CO_2 adsorption capacity. The samples dried at room temperature for 24 h showed higher adsorption capacity (14.2−17 cm^3/g) as compared to samples dried at the higher temperature of 110 °C in an oven for 12 h (12−13.5 cm^3/g) (Figure 6f). Drying at higher temperature causes loss of interlayer water molecules from LDH, resulting a decrease in CO_2 adsorption capacity, while samples dried at ambient temperature have interlayer water molecules to react with CO_2 to form bicarbonates in the presence of water molecules as per the equation $M_2CO_3 + CO_2 + H_2O \rightarrow 2MHCO_3$, which is favorable for adsorption of CO_2 and enhances the adsorption capacity.[25]

LDH samples having higher surface area are expected to show higher adsorption capacity for CO_2, if only physisorption of gas occurs. The present study showed the multilayer adsorption

Table 7. Langmuir Parameters for CO_2 Adsorption on Mg−Al-9 LDH Sample at Different Activation and Adsorption Temperatures

	30 °C			60 °C		
activation temperature (°C)	q ($cm^3\ g^{-1}\ mmHg^{-1}$)	b ($mmHg^{-1}$)	regression (R^2)	q ($cm^3\ g^{-1}\ mmHg^{-1}$)	b ($mmHg^{-1}$)	regression (R^2)
150	18.208	0.0774	0.8540	22.59	0.0365	0.9088
250	11.571	0.0126	0.6922	9.755	0.0160	0.7288
350	10.368	0.0039	0.9446	5.340	0.0345	0.7858

Table 8. Langmuir−Freundlich Parameters for CO_2 Adsorption on Mg−Al-9LDH Sample at Different Activation and Adsorption Temperatures

	30 °C				60 °C			
activation temperature (°C)	q ($cm^3\ g^{-1}\ mmHg^{-1}$)	b ($mmHg^{-n}$)	n	regression (R^2)	q ($cm^3\ g^{-1}\ mmHg^{-1}$)	b ($mmHg^{-n}$)	n	regression (R^2)
150	520.83	0.0915	0.1860	0.9814	263.58	0.0305	0.1716	0.9941
250	1515.97	0.0013	0.2481	0.9292	707.97	0.0026	0.2458	0.9498
350	707.96	0.0005	0.4615	0.9893	41.39	0.0530	0.1547	0.7479

Table 9. Freundlich Parameters for CO_2 Adsorption on Mg−Al-9 LDH Sample at Different Activation and Adsorption Temperatures

	30 °C			60 °C		
activation temperature (°C)	K ($cm^3\ g^{-1}\ mmHg^{-n}$)	n	regression (R^2)	K ($cm^3\ g^{-1}\ mmHg^{-n}$)	n	regression (R^2)
150	6.104	0.1772	0.9814	7.978	0.1596	0.9946
250	2.115	0.2471	0.9295	1.845	0.2476	0.9501
350	0.384	0.4583	0.9895	2.141	0.1378	0.7481

having both chemisorption and physisorption; therefore, no linear correlation of adsorption capacity of CO_2 with the surface area has been observed. On the other hand, higher crystallinity results in well-developed layered structure having CO_3^{2-} anions as basic sites in the interlayer space, resulting in the enhanced chemisorption of CO_2. The sample having higher crystallinity and surface area showed higher chemisorption as well as physisorption; however, the sample having one of the parameters, namely, crystallinity or surface area, lower showed lower adsorption capacity for CO_2 even if the other has a higher value.

Disk diameter was observed to have a correlation with CO_2 adsorption capacity. For example, LDH sample having highest the disk diameter of 51 nm showed a maximum CO_2 adsorption of 22 cm^3/g. Disk diameter represents the width of the brucite layer of LDH sample; therefore, with an increase in disk diameter, the width of the layer increases, which leads to an increase in the number of basic sites as well as interstitial space, which in turn increases the adsorption capacity.

The LDH sample (Mg−Al-9) prepared with optimized synthetic conditions (as discussed above) showed maximum CO_2 adsorption (22 cm^3/g), which was found to be similar with commercial Mg−Al−CO_3 LDH sample (Pural MG63) under similar adsorption conditions of 1 bar and 30 °C (Table 2). After calcination at 500 °C for 4 h, the sample (Mg−Al−C) showed a decrease in CO_2 adsorption (16 cm^3/g).

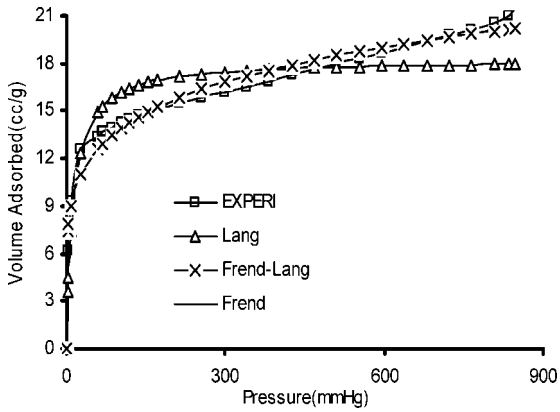

Figure 5. Langmuir, Freundlich, and Langmuir−Freundlich isotherm fittings for CO_2 adsorption on Mg−Al-9 LDH.

The desorption pattern of all LDH samples showed the chemisorption of CO_2 over the LDH surface, as complete desorption of CO_2 does not occur by only changing pressure at the same temperature (Figure 7a−c). However, the calcined LDH sample (Figure 7d) showed complete desorption of CO_2 due to the physisorption of CO_2 over calcined LDH surface. Furthermore, a CO_2 adsorption study at different activation

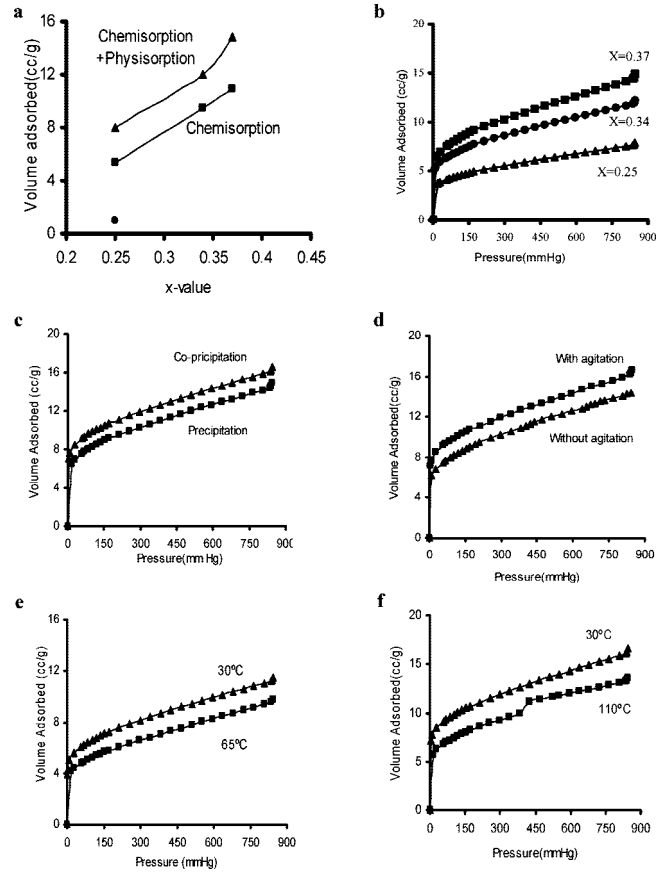

Figure 6. (a) Relation between Al content and CO_2 adsorption capacity. CO_2 adsorption isotherm of Mg−Al−CO_3LDH (b) having different Al content, (c) prepared with precipitation and coprecipitation method (d) prepared with and without agitation, (e) prepared at different addition temperature, and (f) dried at 30 and 110 °C.

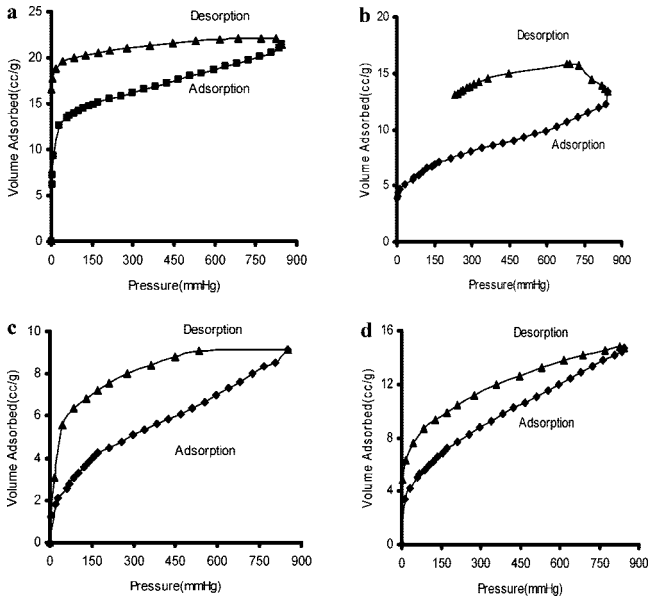

Figure 7. CO_2 Adsorption isotherm of Mg−Al−CO_3 LDH at 30 °C after degassing at different temperatures: (a) 150 °C, (b) 250 °C, (c) 350 °C, and (d) 150 °C.

Table 10. CO_2 Adsorption Capacity of Mg−Al-9 LDH at Different Activation and Adsorption Temperatures

	CO_2 adsorption (cm^3/g)	
activation temperature (°C)	30 °C	60 °C
150	22	23
250	14	12
350	8	8

temperatures (150, 250, and 350 °C) showed a decrease in adsorption capacity from 22 to 8.2 cm^3/g upon increasing the activation temperature from 150 to 350 °C (Table 10). It shows that CO_2 adsorption on Mg−Al−CO_3 LDH is significantly affected by the structural changes occurring during the heating of the material. Heating of the samples at 150 °C results in loss of some of the interlayer water, as TGA data showed the complete removal of interlayer water at ∼200 °C. As small amount of water present helps in the adsorption of CO_2, the LDH samples were observed to show maximum adsorption (22 cm^3/g). However, incomplete desorption occurs due to the chemisorption of CO_2 (Figure 7a). Upon heating at 200−300 °C, interlayer space significantly collapses, as evident by HT-PXRD data (Figure 3), due to dehydration and dehydroxylation of −OH groups bound with Mg^{2+} ions. This increases the availability of Mg^{2+} ions to react with CO_2 to form $MgCO_3$, resulting in chemisorption of CO_2 over the LDH surface.[51] Tichit et al.[52] attributed the progressive collapse of the layered structure and progressive increase in the lattice *a* parameter with increasing temperature due to the migration of Al^{3+} ions from the framework octahedral brucite-type layers to tetrahedral sites in the interlayer. This effectively makes the framework Mg^{2+} ions more accessible to react with CO_2. Therefore, the decrease in d_{003} at higher temperature results in the decrease in adsorption capacity after activation at 250 °C (14 cm^3/g), and the increased chemisorption of CO_2 after activation at 250 °C results in less desorption as compared to desorption after activation at 150 °C (Figure 7b). Further heating at 350 °C results in complete destruction of layered structure, as evident by HT-PXRD data (Figure 3), and the material becomes amorphous, having lower adsorption of CO_2 (8.2 cm^3/g); however, Mg^{2+} ions are less available as compared to the sample heated at 250 °C. Thus, desorption is better than for the sample heated at 250 °C (Figure 7c). Further heating at temperature higher than 400 °C results in the decomposition of CO_3^{2-}, and at this point a three-dimensional structure is formed consisting of a close-packed oxygen network, which traps in its interstices a disordered cation configuration with octahedral (M^{2+}) and tetrahedral (M^{3+}) cations. The decreased availability of Mg favors physisorption over chemisorption at this temperature,[51] which can be clearly seen in the calcined sample (Mg−Al-9) showing complete desorption after activation at 150 °C (Figure 7d).

The CO_2 adsorption study at higher adsorption temperature (60 °C) shows adsorption capacity in a similar range (Table 10); however, desorption was observed to be incomplete due to chemisorption.

4. Conclusions

The CO_2 adsorption capacity of Mg−Al−CO_3 LDH is significantly influenced by the synthetic parameters used during the preparation of the material. Among the various synthetic parameters, cation molar ratio, mode of addition of magnesium and aluminum precursors, addition temperature, agitation, and drying play an important role in the structural and textural features of the material, which further influence its adsorption capacity for CO_2. On the basis of the study, 37% Al content (i.e., 1.7:1 Mg:Al ratio) and room temperature addition of magnesium and aluminum precursors followed by agitation at 65 °C for 18 h and room temperature drying of the material are the optimal conditions for the synthesis of Mg−Al−CO_3 LDH sample, resulting a maximum CO_2 adsorption of 22 cm^3/g, similar to commercial hydrotalcite sample. The adsorption data was found to be best described by the Freundlich isotherm, because experimental data show multilayer adsorption; i.e., the adsorption up to the Langmuir saturation point shows chemisorption and after that physisorption. However, the Langmuir saturation point indicates that, with an increase in Al content, chemisorption also increases linearly. The amount of CO_2 adsorbed in terms of CO_3^{2-} content shows that 1 mol % increase in Al content results to increase 0.5 mol % CO_3^{2-} content. The incomplete desorption isotherm confirms the chemisorption of CO_2 over the LDH surface, whereas the calcined material shows complete desorption due to the destruction of hydrotalcite structure and the reduced availability of Mg^{2+} to form $MgCO_3$ with CO_2, which favor physisorption over chemisorption after calcination at 400−500 °C.

Acknowledgment

Authors are thankful to Director, CSMCRI, for encouragement and to Mr. Ranjeet Pillai for the surface area analysis and CO_2 adsorption study. Authors are thankful to Dr. Pragyana Bhatt for PXRD and Mr. Harish Jirimali for TGA analysis.

Literature Cited

(1) Zhang, J.; Zhang, F.; Ren, L.; Evans, D. G.; Duan, X. Synthesis of layered double hydroxide anionic clays intercalated by carboxylate anions. *Mater. Chem. Phys.* **2004**, *85*, 207.

(2) Rivera, J. A.; Fetter, G.; Bosch, P. Microwave power effect on hydrotalcite synthesis. *Microporous Mesoporous Mater.* **2006**, *89*, 306.

(3) Roussel, H.; Briois, V.; Elkaim, E.; Roy, A. D.; Besse, J. P.; Jolivet, J. P. Study of the formation of the layered double hydroxide [Zn−Cr−Cl]. *Chem. Mater.* **2001**, *13*, 329.

(4) Seftel, E. M.; Dvininov, E.; Lutic, D.; Popovice, E.; Ciocoiu, C. Synthesis of hydrotalcite type anionic clays containing biomolecules. *J. Optoelectron. Adv. Mater.* **2005**, *7*, 2869.

(5) Yong, Z.; Rodrigues, A. E. Hydrotalcite like compounds as adsorbents for carbon dioxide. *Energy Convers. Manage.* **2002**, *43*, 1865.

(6) Xie, X.; An, X.; Wang, X.; Wang, Z. Preparation, characterization and application of ZnAlLa-hydrotalcite like compounds. *J. Nat. Gas Chem.* **2003**, *12*, 259.

(7) Forano, C.; Hibino, T.; Leroux, F.; Gueho, C. T. *Handbook of Clay Science*; Elsevier: New York, 2006.

(8) Schaper, H.; Berg-Slot, J. J.; Stork, W. H. J. Stabilized magnesia: A novel catalyst (support) material. *Appl. Catal.* **1989**, *54*, 79.

(9) McKenzie, A. L.; Fishel, C. T.; Davis, R. J. Investigation of the surface and basic properties of calcined hydrotalcite. *J. Catal.* **1992**, *138*, 547.

(10) Yu, J. J.; Jiang, Z.; Zhu, L.; Hao, Z. P.; Xu, Z. P. Adsorption/desorption studies of NO_X on well mixed oxides derived from Co−Mg/Al hydrotalcite like compounds. *J. Phys. Chem. B* **2006**, *110*, 4291.

(11) Cantu, M.; Salinas, E. L.; Valante, J. S. SO_X removal by calcined MgAlFe hydrotalcite like materials: Effect of the chemical composition and cerium incorporation method. *Environ. Sci. Technol.* **2005**, *39*, 9715.

(12) Soares, J. L.; Moreira, R. F. P. M.; Jose, H. J.; Grande, C. A.; Rodrigues, A. E. Hydrotalcite materials for CO_2 adsorpion at high temperatures: Characterization and diffusivity measurements. *Sep. Sci. Technol.* **2004**, *39*, 1989.

(13) Yamamoto, T.; Kodama, T.; Hasegawa, N.; Tsuji, M.; Tamaura, Y. Synthesis of hydrotalcite with high layer charge for CO_2 adsorbent. *Energy Convers. Manage.* **1995**, *36*, 637.

(14) Dousova, B.; Machovic, V.; Kolousek, D.; Kovanda, F.; Dornicak, V. Sorption of As(v) species from aqueous systems. *Water, Air, Soil Pollut.* **2003**, *149*, 251.

(15) Das, N. N.; Konar, J.; Mohanta, M. K.; Srivastava, S. C. Adsorption of Cr (VI) and Se(IV) from their aqueous solutions onto Zr^{4+} substituted ZnAl /MgAl layered double hydroxides: Effect of Zr^{4+} substitution in the layer. *J. Colloid Interface Sci.* **2004**, *270*, 1.

(16) Wang, H.; Chen, J.; Cai, Y.; Ji, J.; Liu, L. H.; Teng, H. Defluoridation of drinking water by Mg/Al hydrotalcite like compounds and their calcined products. *Appl. Clay Sci* **2007**, *35*, 59.

(17) Sels, B. F.; De Vos, D. E.; Jacobs, P. A. Hydrotalcite like anionic clays in catalytic organic reactions. *Cat. Rev.* **2001**, *43*, 443.

(18) Choudary, B. M.; kantam, M. L.; Reddy, Ch. V.; Rao, K. K.; Figueras, F. Henry reactions catalysed by modified Mg−Al hydrotalcite: An efficient reusable solid base for selective synthesis of β- nitroalkanols. *Green Chem.* **1999**, *1*, 187.

(19) Choudary, B. M.; Kantam, M. L.; Reddy, C.; Rao, K. K.; Figueras, F. The first example of michael addition catalysed by modified Mg−Al hydrotalcite. *J. Mol. Catal. A: Chem.* **1999**, *146*, 279.

(20) Cwik, A.; Fuchs, A.; Hell, Z.; Clacens, J. M. An efficient and environmental friendly synthesis of 4-hydroxy-arylpiperidines using hydrotalcite catalyst. *J. Mol. Catal. A: Chem.* **2004**, *219*, 377.

(21) Reynolds, S. P.; Ebner, A. D.; Ritter, J. A. New pressure swing adsorption cycles for carbon dioxide sequestration. *Adsorption* **2005**, *11*, 531.

(22) Mao, G.; Tsuji, M.; Tamaura, Y. Synthesis and CO_2 adsorption features of a hydrotalcite like compound of the $Mg^{2+}-Al^{3+}-Fe(CN)_6^{4-}$ system with high layer charge density. *Clays Clay Miner.* **1993**, *41*, 731.

(23) Herzog, H.; Drake, E.; Adams, E. CO_2 capture, reuse, and storage technologies for mitigating global climate change. DOE/DE-AF22-96PC01257, 1997.

(24) Ruther, J. A. FETC programs for reducing greenhouse gas emissions. DOE/FETC-98/1058, 1999.

(25) Yong, Z.; Mata, V.; Rodrigues, A. E. Adsorption of carbon dioxide onto hydrotalcite like compounds (HTlcs) at high temperature. *Ind. Eng. Chem. Res.* **2001**, *40*, 204.

(26) Soares, J. L.; Casarin, G. L.; Jose, H. J.; De, R.; Moreira, F. P. M. Experimental and theoretical analysis for the CO_2 adsorption on hydrotalcite. *Adsorption* **2005**, *11*, 237.

(27) Iwan, A.; Lapkin, A. Development of CO_2 adsorbent and reagents for sorption enhanced methane steam reforming. *Proceedings of the International Hydrogen Energy Congress and Exhibition IHEC*; 2005; 13−15.

(28) Reijers, H. Th. J.; Valster-Schiermeier, S. E. A.; Cobden, P. D.; van den Brink, R. W. Hydrotalcite as CO_2 sorbent for sorption-enhanced steam reforming of methane. *Ind. Eng. Chem. Res.* **2006**, *45*, 2522.

(29) White, M. G.; Iretskii, A. V.; Weigel, J. S.; Chiang, R. L.; Brozozowski, J. R. Adsorbents, methods of preparation, and methods of use thereof. International Patent no. WO2004/000440 A1, 2003.

(30) Prinetto, F.; Ghiotti, G.; Graffin, P.; Tichit, D. Synthesis and characterization of sol-gel Mg/Al and Ni/Al layered double hydroxides and comparison with co-precipitated samples. *Microporous Mesoporous Mater.* **2000**, *39*, 229.

(31) Tichit, D.; Lorret, O.; Coq, B.; Prinetto, F.; Ghiotti, G. Synthesis and characterization of Zn/Al and Pt/Zn/Al layered double hydroxides obtained by the solgel method. *Microporous Mesoporous Mater.* **2005**, *80*, 213.

(32) Jitianu, M.; Zaharescu, M.; Balasoiu, M.; Jitianu, A. The solgel route in synthesis of Cr (III) containing clays. Comparison between Mg-Cr and Ni-Cr anionic clays. *J. Sol-Gel Sci. Technol.* **2003**, *26*, 217.

(33) Rao, M. M.; Reddy, B. R.; Jayalakshmi, M.; Jaya, V. S.; Sridhar, B. Hydrothermal synthesis of Mg-Al hydrotalcites by urea hydrolysis. *Mater. Res. Bull.* **2005**, *40*, 347.

(34) Kanezaki, E. Effect of atomic ratio Mg/Al in layers of Mg and Al layered double hydroxide on thermal stability of hydrotalcite-like layered structure by means of in situ high temperature powder X-ray diffraction. *Mater. Res. Bull.* **1998**, *33*, 773.

(35) Kim, Y.; Yang, W.; Liu, P. K. T.; Sahimi, M.; Tsotsis, T. T. Thermal evolution of the structure of a Mg-Al-CO_3 layered double hydroxide: Sorption reversibility aspects. *Ind. Eng. Chem. Res.* **2004**, *43*, 4559.

(36) Yang, W.; Kim, Y.; Liu, P. K. T.; Sahimi, M.; Tsotsis, T. T. A study by in situ technique of the thermal evolution of the structure of a Mg-Al-CO_3 layered double hydroxide. *Chem. Eng. Sci.* **2002**, *57*, 2945.

(37) Kovanda, F.; Grygar, T.; Dornicak, V.; Rojka, T.; Bezdicka, P.; Jiratova, K. Thermal behaviour of Cu-Mg-Mn and Ni-Mg-Mn layered double hydroxides and characterization of formed oxides. *Appl. Clay Sci.* **2005**, *28*, 121.

(38) Ramirez, J. P.; Mul, G.; Kapteijn, F.; Moulijn, J. A. A spectroscopic study of the effect of the trivalent cation on the thermal decomposition behaviour of Co-based hydrotalcites. *J. Mater. Chem.* **2001**, *11*, 2529.

(39) Yong, Z.; Mata, V.; Rodrigues, A. E. Adsorption of carbon dioxide at high temperature−sA review. *Sep. Purif. Technol.* **2002**, *6*, 195.

(40) Ding, Y.; Alpay, E. Equilibria and kinetics of CO_2 adsorption on hydrotalcite adsorbent. *Chem. Eng. Sci.* **2000**, *55*, 3461.

(41) Othman, M. R.; Rasid, N. M.; Fernando, W. J. N. Mg-Al hydrotalcite coating on zeolites for improved carbon dioxide adsorption. *Chem. Eng. Sci.* **2006**, *61*, 1555.

(42) Ebner, A. D.; Reynolds, S. P.; Ritter, J. A. Understanding the adsorption and desorption behavior of CO_2 on a K-promoted hydrotalcite-like compound (HTlc) through nonequilibrium dynamic isotherms. *Ind. Eng. Chem. Res.* **2006**, *45*, 6387.

(43) Ebner, A. D.; Reynolds, S. P.; Ritter, J. A. Nonequilibrium kinetic model that describes the reversible adsorption and desorption behavior of CO_2 in a K-promoted hydrotalcite like compound. *Ind. Eng. Chem. Res.* **2007**, *46*, 1737.

(44) Ficicilar, B.; Dogu, T. Breakthrough analysis for CO_2 removal by activated hydrotalcite and soda ash. *Catal. Today* **2006**, *115*, 274.

(45) Cullity, D.; Stock, S. R. *Elements of X-ray Diffraction*, 3rd ed.; Prentice Hall: Upper Saddle River, NJ, 2001.

(46) Gregg, S. J.; Sing, K. S. W. *Adsorption, Surface Area and Porosity*, 2nd ed; Academic Press: New York, 1982.

(47) Yang, R. T. *Gas Separation by Adsorption Process*, Imperial College Press: London, 1997.

(48) Masel, R. I. *Principles of Adsorption and Reaction on Solid Surfaces*; Wiley-Interscience: New York, 1996.

(49) Thomas, G. S.; Rajamurthi, M.; Kamath, P. V. DIFFaX simulations of polytypism and disorder in hydrotalcite. *Clays Clay Miner.* **2004**, *52*, 693.

(50) Millange, F.; Walton, R. I.; O'Hare, D. Time resolved in situ X-ray diffraction study of the liquid phase reconstruction of Mg−Al carbonate hydrotalcite like compounds. *J. Mater. Chem.* **2000**, *10*, 1713.

(51) Huston, N. D.; Speakman, S. A.; Payzant, E. A. Structural effects on the high temperature adsorption of CO_2 on a synthetic hydrotalcite. *Chem. Mater.* **2004**, *16*, 4135.

(52) Tichit, D.; Bennani, M. N.; Figueras, F.; Ruiz, J. R. Decomposition processes and characterization of the surface basicity of Cl^- and CO_3^{2-} hydrotalcites. *Langmuir* **1998**, *14*, 2086.

Received for review March 5, 2008
Revised manuscript received August 14, 2008
Accepted September 15, 2008

IE800365T